Chemical Physics 539 (2020) 110973

Contents lists available at ScienceDirect

Chemical Physics

journal homepage: www.elsevier.com/locate/chemphys

# Photoelectron spectroscopy studies of PTCDI on Sn/Si(111)-$2\sqrt{3} \times 2\sqrt{3}$

C. Emanuelsson, L.S.O. Johansson, H.M. Zhang*

*Department of Engineering and Physics, Karlstad University, SE-651 88 Karlstad, Sweden*

ARTICLE INFO

*Keywords:*
PTCDI
UPS
XPS
NEXAFS
Electronic structure
Metal/semiconductor surface

ABSTRACT

3,4,9,10-perylene tetracarboxylic diimide molecules were evaporated onto a Sn/ Si(111)-$2\sqrt{3} \times 2\sqrt{3}$ surface and studied using photoelectron spectroscopy and near edge X-ray absorption fine structure (NEXAFS). We found evidences of a strong interaction between the PTCDI molecules and the substrate. The interactions cause changes in the Sn 4d, C 1s, and N 1s core level spectra. These interactions also cause a complete absence of transitions to the lowest unoccupied molecular orbital (LUMO) in the NEXAFS spectra, in combination with a new state between the regular highest occupied molecular orbital (HOMO) and the Fermi level at low coverages. These changes are explained to be due to the charge transfer from the top Sn atoms to the PTCDI molecules, resulting in a split of the HOMO, and lowering of the LUMO levels. The interactions are shown to heavily involve the carbonyl carbon and partly nitrogen atoms of the imide group.

## 1. Introduction

The last few decades, thin films of organic semiconductors have received growing attention from the scientific community since they show promising properties for use in electronic devices. The performance of these devices are strongly dependent on the structure and quality of the thin films. The interface between the substrate and the molecular film is of special interest since it influences the growth of the entire film. To understand the interface it is important to characterize the molecule/substrate interactions and the intermolecular interactions, and their relative strength, since they determine the morphology and electronic structure of the interface.

Previously, the perylene derivative 3,4,9,10-perylene tetracarboxylic dianhydrid (PTCDA) has been used as a model molecule for self-assembled molecular films. To further understand the interactions involved in the growth of large $\pi$-conjugated molecules on substrates, it is important to study similar molecules as PTCDA but with different endgroups. One such molecule, 3,4,9,10-perylene tetracarboxylic diimide (PTCDI), has recently attracted attention since it can be functionalized through its endgroups to tune its properties [1]. A ball and stick model of the PTCDI molecule is presented in Fig. 1 where different carbon atoms have been numbered as C1–C7 for later convenience. The electronic structure of thin PTCDI films has previosuly been studied using ultraviolet photoelectron spectroscopy (UPS), X-ray photoelectron spectroscopy (XPS) and near edge X-ray absorption fine structure (NEXAFS) on Si(111) [2], Ni(111) [2], Au(111) [3,4], Ag(111) [4], Cu (111) [4], $TiO_2$ [5,6] and Ag/Si(111)-$\sqrt{3} \times \sqrt{3}$ [7].

The Sn/Si(111)-$2\sqrt{3} \times 2\sqrt{3}$ surface, henceforth Sn-$2\sqrt{3}$, is a metal-induced reconstruction formed at a Sn coverage above 1 monolayer (ML) [8–11]. There is to this date no consensus about the exact atomic configuration of the surface. Scanning probe microscopy studies and photoelectron spectroscopy studies suggest that the surface has a double layer of Sn atoms, a top layer consisting of two inequivalent Sn-pairs and a bottom layer consisting of 8–10 Sn atoms [8–12]. The simpler Sn/Si(111)- surface contains dangling bonds which causes a strong chemical reaction that causes the PTCDA to stand up on the surface, which does not allow for ordered growth at low coverages [13]. The extra layer of Sn atoms in the Sn-$2\sqrt{3}$ surface passivates the dangling bonds and allows for the formation of interesting ordered structures at low coverages.

In a previous work, we studied PTCDI on Sn/Si(111)-$2\sqrt{3} \times 2\sqrt{3}$ using scanning tunneling microscopy (STM) and low energy electron diffraction (LEED). At low coverages single molecules could be found on the substrate, indicating a strong substrate/molecule interaction. The molecules also formed 1D rows which became more dominant with increasing coverages up to about 0.5 ML. Meanwhile, parallel rows with a $4\sqrt{3}$ distance between them formed patches of a commensurate $4\sqrt{3} \times 2\sqrt{3}$ reconstruction. At coverages close to 1 ML the PTCDI molecules were found to form several 2D structures and above 1 ML coverage the molecular growth was characterized as island growth [14]. In this paper we have studied the same system, PTCDI on Sn/Si (111)-$2\sqrt{3} \times 2\sqrt{3}$, using UPS, XPS and NEXAFS to further investigate the electronic structures and clarify the interactions involved in this interface.

* Corresponding author.
*E-mail address:* hanmin.zhang@kau.se (H.M. Zhang).

https://doi.org/10.1016/j.chemphys.2020.110973
Received 17 April 2020; Received in revised form 28 August 2020; Accepted 30 August 2020
Available online 06 September 2020

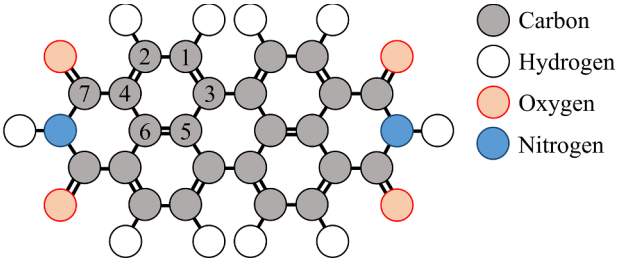


**Fig. 1.** The PTCDI molecule with different carbon atoms numbered from 1 to 7.

## 2. Experimental details

The experiment was performed at beamline I311 at the MAX-lab synchrotron radiation facility in Lund, Sweden [15]. The endstation was equipped with a Scienta SES200 electron analyzer. The photoelectron spectra were recorded using measurement parameters that gave energy resolutions about ~20 meV for the valence band, Si 2p and Sn 4d spectra, ~75 meV for C 1s, and ~100 meV for O 1s and N 1s. The photon energies used for these spectra were 60 eV for the valance band, 140 eV for Si 2p, 80 eV for Sn 4d, 350 eV for C 1s and 600 eV for both O 1s and N 1s. Auger electron yield (AEY) NEXAFS spectra were measured using the SES200 as an electron detector, at the C, O and N adsorption edges. The samples used were Shiraki-etched [16] Si(111), B-doped to a resistivity of 0.7–1.5 Ωcm. The oxide was removed by stepwise resistive heating up to 940 °C. The Sn/Si(111)-$2\sqrt{3} \times 2\sqrt{3}$ reconstruction was created in two steps. In the first step a $\sqrt{3} \times \sqrt{3}$ surface was created by evaporating 0.3 ML Sn onto the Si(111) substrate followed by annealing at 600 °C. In the second step the $2\sqrt{3} \times 2\sqrt{3}$ surface was created by evaporating 1.1 ML extra Sn onto the surface followed by annealing at 300 °C, which resulted in a sharp $2\sqrt{3} \times 2\sqrt{3}$ LEED pattern. The surface quality was also checked using core level spectra. 1 ML Sn is defined as the coverage at which there is one Sn atom for each lattice point of Si (111) while 1 ML PTCDI is defined as the coverage at which the surface is covered by the canted phase of PTCDI. PTCDI was evaporated using a Knudsen cell held at 300 °C, while the substrates were held at room temperature (RT). Several PTCDI coverages from 0.5 ML to 5.0 ML were studied and all data presented here were measured at RT. In the peakfits, the backgrounds for Sn 4d, C 1s, O 1s and N 1s were reduced with a Shirley function. A Voigt type core level profile was used for the various components. The Lorentzian width was fixed to 175 meV for Sn 4d and 100 meV for O-, N-, and C 1s while the Gaussian widths were fitted in each case.

## 3. Results

### 3.1. Si 2p and Sn 4d core level spectra

There was no apparent change in the lineshape or energy position of the peaks in the Si 2p core level spectra (aviable as supplementary material) when PTCDI was deposited onto the surface.

The Sn 4d spectra for different PTCDI coverages are presented in Fig. 2. The clean substrate spectrum shows two distinct spin orbit peaks, each having a shoulder on the high binding energy (BE) side. When PTCDI was evaporated onto the Sn-$2\sqrt{3}$ surface a new, distinct shoulder shows up on the higher BE side of the substrate related peaks, at about 25.8 eV. To investigate these changes in more detail the spectra have been analyzed by fitting of components and the presented results have had an integrated Shirley background removed. The peak-fit parameters are presented in Table 1.

The spectra were fitted using spin–orbit split components with a split of 1.05 eV and branching ratio of 0.75. The spectrum recorded at the clean substrate shown in Fig. 2a) was fitted using two components *a* and *b*, located at BE 24.04 and 24.37 eV, respectively. After deposition of PTCDI a third component *c* is required to fit the new surface. At 0.5 ML PTCDI coverage the component *c* is located at 0.67 eV higher BE with respect to component *a* and has a relative intensity of 19.64%. The component *a* loses 38.27% and *b* gains 18.00% respectively compared to the clean Sn-$2\sqrt{3}$ surface. The BE positions of the components *a* and *b* do not change significantly after the PTCDI deposition, only component *b* shifts about 0.16 eV towards lower BE when the first 0.5 ML were deposited. With further PTCDI deposition there are minor changes in the spectra compared to the one at 0.5 ML coverage. At 2.5 ML the components *a*, *b* and *c* have relative intensities of 41.77, 36.21 and 23.02% respectively.

### 3.2. C 1s core level spectra

C 1s spectra recorded at different PTCDI coverages are presented in Fig. 3, where each spectrum has been fitted and an integrated Shirley background has been removed from them. The multilayer spectrum in Fig. 3d) involves two main features, the strongest of which sits at a BE position of about 285.0 eV while the smaller one is located at 288.5 eV. The larger and smaller features have previously been assigned to carbons from the perylene core and the imide endgroup, respectively [4]. The spectrum also contains a number of shakeups on the higher BE side of the main feature. At low coverages however, the situation is significantly different as seen in the spectrum recorded at a PTCDI coverage of 0.5 ML, presented in Fig. 3a). The feature related to the perylene core sits at lower BE and the imide related feature (*d*) is less intense while the shakeup (*e*) between the larger and the smaller feature is much more intense, compared to the 5.0 ML spectrum.

To study these changes in more detail, the spectra were analyzed by fitting of components. The 5.0 ML spectrum can be fitted with seven components labeled as *a-g*. The perylene related feature was fitted using three components *a-c* as in previous work [4,7,17], where *a* corresponds to C–H (C1 and C2 in Fig. 1), *b* to C–C (C3, C5 and C6) and *c* to C–C = O (C4). The carbon in the imide group (C7) was fitted with the component *d*. The shakeup features were fitted with components *e–g*, respectively. The 5.0 ML spectrum was regarded as a reference and it was verified that the fitting of it indeed gave the components (*a,b,c*) the ratios (8,8,4) according to the stoichiometry of the perylene core of PTCDI. Also, the *b*-component was allowed to have slightly higher Gaussian width than the other main components, since C1 and C2 have been calculated to be separated in BE by 0.2 eV [5]. For the lower coverages the eighth component *h* was necessary in order to obtain acceptable results from the fitting analysis. This component is situated between the perylene related feature and its shakeup, *e*. The fitting parameters for the peakfits of the C 1s spectra are presented in Table 2.

The peakfit shows that the components of the perylene core indeed shift towards higher BE with increasing PTCDI coverages. Component *a* shifts the most by 0.55 eV while *b* and *c* shift about 0.25 and 0.2 eV respectively. The intensity of components *d* and *e* also have an interesting behaviour with respect to coverages. The imide related component *d*, only has a relative intensity of 2% at 0.5 ML, which increases to 8% at 5.0 ML. On the other hand, component *e* which usually is associated with a shakeup is more intense at low coverages and has a relative intensity of 9% at 0.5 ML, which decreases to about 3.4% at 5.0 ML. Except the changes in relative intensity the components *d* and *e* are fairly stable in BE positions. Component *d* shifts 0.14 and *e* shifts 0.07 eV towards lower BE with increasing PTCDI coverages, respectively. Except the already mentioned changes with PTCDI coverages there is also a component *h* that is only found at low coverages located at a BE of about 295.9 eV. This component has a relative intensity of 7.2% at 0.5 ML and loses intensity very quickly with increasing PTCDI coverages. At 1.5 ML it only has about 2.5% and above that coverage the component is barely needed to get satisfactory results from the fitting as seen in Table 2.

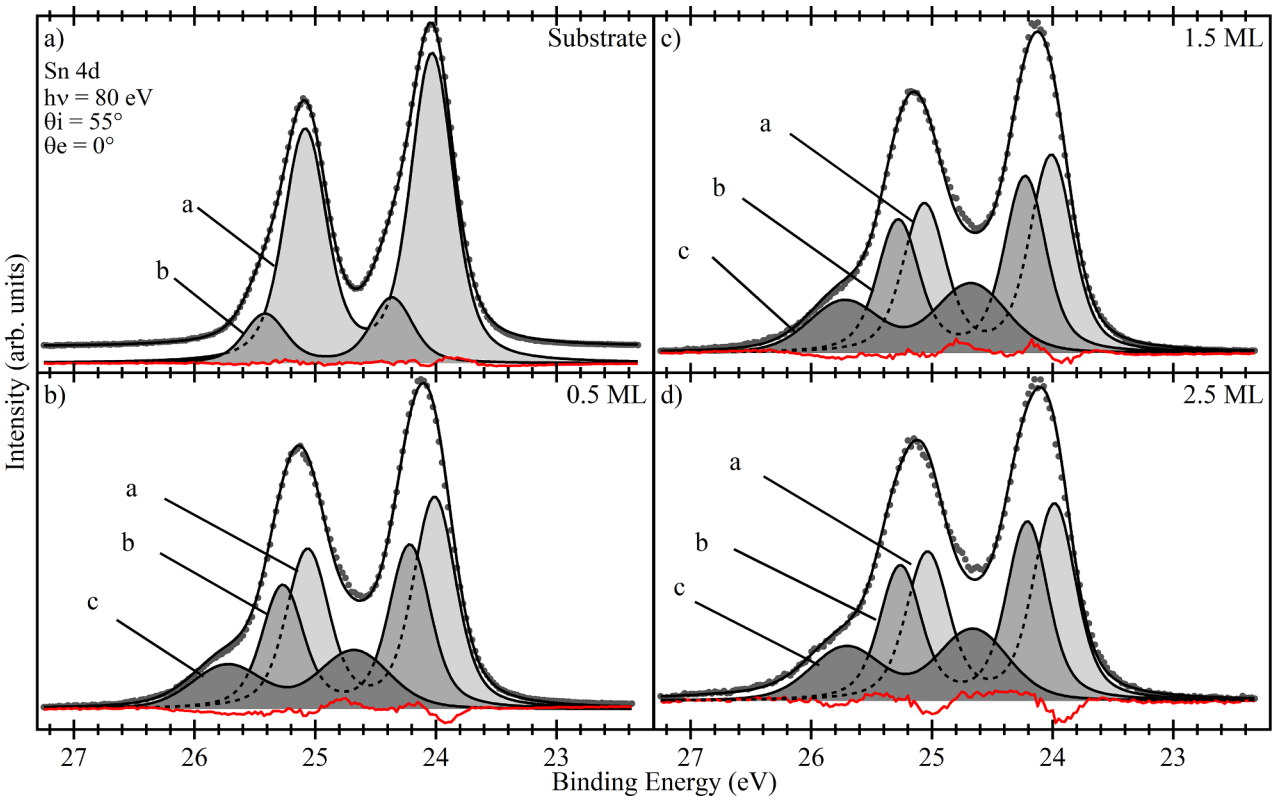


**Fig. 2.** Peakfits of Sn 4d core level spectra for four thicknesses of PTCDI on Sn/Si(111)-$2\sqrt{3} \times 2\sqrt{3}$. The measured data with Shirley background removed is plotted with grey dots. The result from the peakfit is plotted as a solid black line. Each fitted component is labelled as a–c and plotted with a filled, solid line. The residual is plotted as a solid red line.

### 3.3. O and N 1s core level spectra

O 1s spectra recorded at different PTCDI coverages are presented in Fig. 4. The spectra only contain two features. The main feature is related to the oxygen atoms in the imide group and the second one is a shakeup associated with the main feature. The main and shakeup features have been fitted with the two components *a* and *b*, respectively and the fitting parameters for the O 1s spectra are presented in Table 3. At 0.5 ML PTCDI coverage the main and second component are at BE of 531.4 and 533.6 eV respectively. The oxygen O 1s spectra exhibit very small changes with respect to PTCDI coverages, i.e. the main feature shifts 0.2 eV towards higher BE from 0.5 to 2.5 ML coverage while the shakeup is at the same BE at all coverages. The relative intensity of the two features also changes slightly with coverages. At 0.5 ML the shakeup has a relative intensity of 11.6%, which increases to 19.1% at 5.0 ML.

N 1s spectra recorded at different PTCDI coverages are presented in Fig. 5. Each spectrum has been fitted and an integrated Shirley background has been removed from them. All spectra involve three features, the strongest of which, the main feature, has a BE of about 400.5 eV. Besides, there is a relatively strong feature at the low BE side of the main feature. This extra feature is positioned about 2 eV below the main feature in BE. In addition, there is also a relatively weak feature at about 2 eV higher binding energy than the main feature, and this is a shakeup of the main feature [4]. The main, extra and shakeup features have been fitted with the three components *a–c*, respectively and the fitting parameters for the N 1s spectra are presented in Table 4.

The fitting shows that the main feature shifts 0.11 eV towards lower BE with increasing PTCDI coverages, and this shift is more or less saturated at 1.5 ML coverage. The extra feature on the other hand shifts more, about 0.43 eV and towards higher BE with increasing coverages. The extra feature is relatively strong at 0.5 ML with an relative intensity of 17.4% and it decreases with increasing coverages to 9.7% at 2.5 ML coverage. This change in component *b* is accompanied by the inverse behaviour in component *a*, which increases from 77.6% at 0.5 ML to 84.6% at 2.5 ML coverage. Then, from 2.5 to 5.0 ML the tendency that was exhibited up to 2.5 ML is reversed and the relative intensity of component *b* increases to 18.8% while component *a* decreases to 74.1%.

### 3.4. NEXAFS

The C K-edge NEXAFS spectra recorded using different incidence angles (available as supplementary material) showed a strong

**Table 1**
Fitting parameters for the components used in the Sn 4d peakfit shown in Fig. 4. The table contains binding energy $E_B$ (eV), relative integrated intensity $I_{rel}$ and the FWHM ($W_G$) of the Gaussian (eV). The Lorentzian width (FWHM), spin–orbit splitting and branch ratio were set to 0.175 eV, 1.05 eV and 0.75 respectively.

| | Substrate | | | 0.5 ML | | | 1.5 ML | | | 2.5 ML | | |
|---|---|---|---|---|---|---|---|---|---|---|---|---|
| | $E_B$ | $I_{rel}$ | $W_G$ | $E_B$ | $I_{rel}$ | $W_G$ | $E_B$ | $I_{rel}$ | $W_G$ | $E_B$ | $I_{rel}$ | $W_G$ |
| a | 24.04 | 83.94% | 0.31 | 24.01 | 45.67% | 0.31 | 24.01 | 41.38% | 0.31 | 23.99 | 40.77% | 0.31 |
| b | 24.37 | 16.06% | 0.30 | 24.21 | 34.66% | 0.30 | 24.23 | 36.10% | 0.30 | 24.21 | 36.21% | 0.30 |
| c | – | – | – | 24.68 | 19.65% | 0.59 | 24.68 | 22.52% | 0.59 | 24.66 | 23.02% | 0.59 |

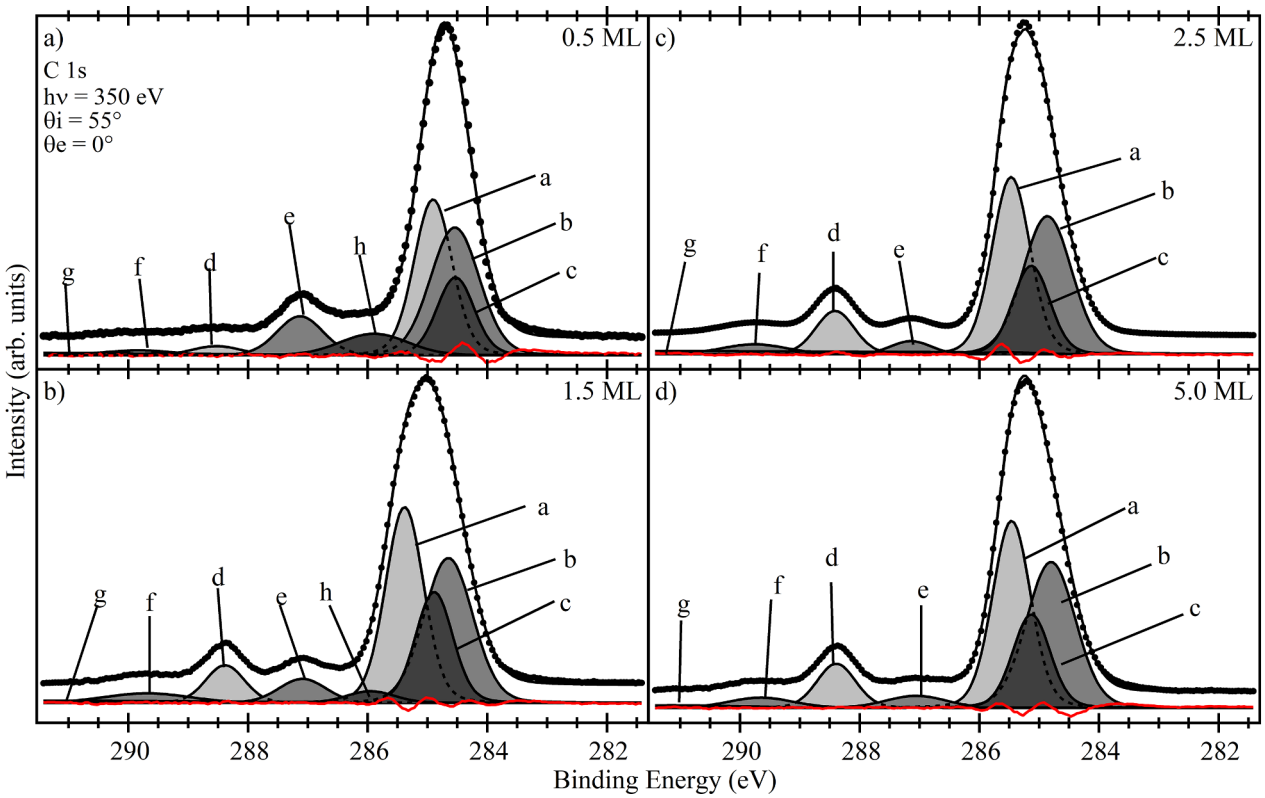


**Fig. 3.** Peakfits of C 1s core level spectra for four thicknesses of PTCDI on Sn/Si(111)-$2\sqrt{3} \times 2\sqrt{3}$. The measured data with Shirley background removed is plotted with black dots. The result from the peakfit is plotted as a solid black line. Each fitted component is labelled as a–h and plotted with a solid line. The residual is plotted as a solid red line.

dependence on the incidence angles. The strong $\pi^*$ resonances at grazing incidence are heavily suppressed at normal incidence, indicating a flat adsorption geometry for the molecules. C K-edge spectra recorded at different PTCDI coverages at incidence angle 70° are presented in Fig. 6. In the spectra there are three groups of sharp features between 283 and 289 eV, which are $\pi^*$-derived resonances [2]. These features have been marked with dashed lines in Fig. 6 and are denoted as *A*–*C*.

Group *A* has previously been described as transitions from the perylene core (C1–C6) to the LUMO (lowest unoccupied molecular orbital) and group *B* as transistions from the same carbon atoms to higher unoccupied orbitals [2]. The three peaks in group *C* are transitions from the carbons in the imide group to various unoccupied states; The first peak is assigned to transitions to LUMO, the second to LUMO + 1. The last peak is a transition to even higher unoccupied orbitals. Comparing the spectra at different PTCDI coverages in Fig. 6 it is clear that several resonances are weaker at low coverages. The features in group *A* and *B* are all weaker in the 0.5 ML spectrum. The first resonance in the group *A* is basically gone at 0.5 ML and becomes of equal strength to the second resonance in the same group at a coverage of 5.0 ML. The features in group *C* clearly shift their positions to higher photon energies with increased coverages.

In Fig. 7 the O K-edge spectra recorded at different coverages with an incidence angle of 70° are presented. The spectra contain two main features at photon energies of 531 and 532.1 eV, which have been denoted as *a* and *b*. The feature *a* and *b* are $\pi^*$-derived resonances to LUMO and LUMO + 1 respectively [2]. The first resonance in the O K-edge spectra shows a strong dependence on the PTCDI coverages as the feature *a* is not present at 0.5 ML coverage and becomes stronger than component *b* after 2.5 ML has been deposited.

The N K-edge spectra (aviable as supplementary material) only contain one $\pi^*$-derived resonance which is located at a photon energy of 400.7 eV. This resonance is to LUMO + 1 since transitions to LUMO is symmetry forbidden [2]. The N K-edge spectra do not show any significant change with PTCDI coverages.

**Table 2**
Fitting parameters for the components used in the C 1s peakfit shown in Fig. 3. The table contains binding energy $E_B$ (eV), relative integrated intensity $I_{rel}$ and the FWHM ($W_G$) of the Gaussian (eV).

| | 0.5 ML | | | 1.5 ML | | | 2.5 ML | | | 5.0 ML | | |
|---|---|---|---|---|---|---|---|---|---|---|---|---|
| | $E_B$ | $I_{rel}$ | $W_G$ | $E_B$ | $I_{rel}$ | $W_G$ | $E_B$ | $I_{rel}$ | $W_G$ | $E_B$ | $I_{rel}$ | $W_G$ |
| a | 284.90 | 30.02% | 0.69 | 285.38 | 32.87% | 0.69 | 285.47 | 31.33% | 0.69 | 285.46 | 32.22% | 0.69 |
| b | 284.54 | 31.27% | 0.91 | 284.65 | 30.87% | 0.94 | 284.86 | 31.04% | 0.91 | 284.80 | 33.45% | 0.91 |
| c | 284.53 | 14.67% | 0.68 | 284.89 | 18.19% | 0.68 | 285.13 | 15.32% | 0.68 | 284.71 | 16.50% | 0.68 |
| d | 288.53 | 2.23% | 0.90 | 288.38 | 6.42% | 0.71 | 288.41 | 7.80% | 0.71 | 288.39 | 8.08% | 0.71 |
| e | 287.13 | 9.00% | 0.85 | 287.09 | 4.94% | 0.86 | 287.14 | 2.46% | 0.73 | 287.06 | 3.39% | 1.13 |
| f | 289.83 | 1.71% | 1.34 | 289.69 | 3.53% | 1.64 | 289.34 | 3.03% | 1.24 | 289.65 | 3.07% | 1.21 |
| g | 291.77 | 3.87% | 6.90 | 291.19 | 3.18% | 7.28 | 290.83 | 8.45% | 1.22 | 291.16 | 1.65% | 2.78 |
| h | 285.89 | 7.23% | 1.28 | 285.95 | 2.46% | 0.89 | 285.54 | 0.05% | 1.16 | – | – | – |

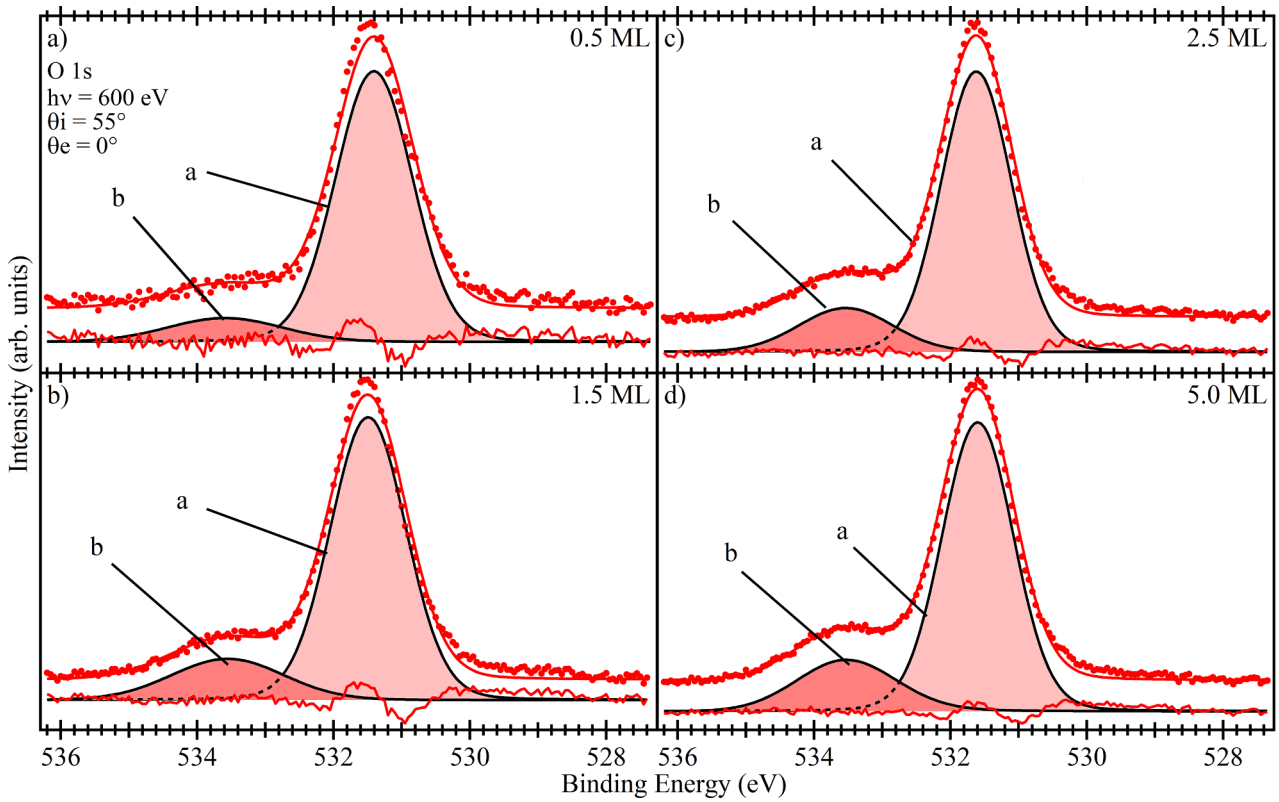


**Fig. 4.** Peakfits of O 1s core level spectra for four thicknesses of PTCDI on Sn/Si(111)-2$\sqrt{3}$ × 2$\sqrt{3}$. The measured data with Shirley background removed is plotted with red dots. The result from the peakfit is plotted as a solid black line. Each fitted component is labelled as a and b, plotted with a filled, solid line. The residual is plotted as a solid red line.

### 3.5. Valence band UPS

The UPS spectra recorded on the clean substrate and different PTCDI coverages using a photon energy of 60 eV are presented in Fig. 8. All spectra recorded when molecules are on the substrate, have a feature at about 2.3 eV, which is close to where the HOMO levels for PTCDI have previously been found [7,18]. At 0.5 and 1.5 ML coverages there is also a state at 1.1 eV below the Fermi level which is denoted as HOMO' in Fig. 8.

## 4. Discussion

Various spectra show changes at submonolayer coverages, indicating an interaction between the Sn-2$\sqrt{3}$ surface and the PTCDI molecules. One of the exceptions is Si 2p, in which the lineshapes and the BE positions of the core level peaks do not change when PTCDI was evaporated onto the substrate. This is somewhat expected as the Si(111) substrate is covered by a bilayer of Sn-atoms, and the interaction with the molecules should only involve the Sn-atoms. The stability of the BE positions of the Si 2p peaks does however show that no band bending occurs when the molecules are deposited onto the Sn-2$\sqrt{3}$ surface.

The other substrate related core level, Sn 4d, is quite interesting as it shows significant changes when PTCDI was evaporated. The spectrum for the clean substrates involves two components. The minor component *b* is regarded to be due to two top Sn atoms with a charge deficit while the majority component *a* is regarded to be due to the remaining two top Sn atoms in combination with the Sn atoms in the first layer [10,19]. In the fitting analysis it was found that the *a*/*b* intensity ratio for the clean substrate is about 5.2. According to the 12 Sn-atom model [11] with 8 Sn-atoms in the first layer and 4 Sn-atoms in the two top inequivalent pairs, the ratio should then be (8 + 2)/2 = 5, which fits well with our results.

The molecule/substrate interaction results in several changes in the Sn 4d core levels, as can be seen in the 0.5 ML spectrum in Fig. 2b). There is a new component *c* and at the same time the component *a* loses a lot of its relative intensity while *b* increases in intensity, compared to the one in the clean substrate. With further PTCDI depositions the situation does not change much, which would suggest that the changes observed in the Sn 4d spectra are saturated just after the first monolayer coverage.

It is evident that Sn donates charge to PTCDI as the extra component *c* sits at a higher BE and the increase of component *b* at the cost of a reduction in component *a*, which sits at the lowest BE. The relative intensity of component *c* saturates close to 25%, which corresponds to 3 Sn atoms. This would suggest that 3 Sn atoms donate charge to PTCDI and consequently are shifted to higher BE and form the component *c*. It

**Table 3**
Fitting parameters for the components used in the O 1s peakfit shown in Fig. 4. The table contains binding energy $E_B$ (eV), relative integrated intensity $I_{rel}$ and the FWHM ($W_G$) of the Gaussian (eV).

| | 0.5 ML | | | 1.5 ML | | | 2.5 ML | | | 5.0 ML | | |
|---|---|---|---|---|---|---|---|---|---|---|---|---|
| | $E_B$ | $I_{rel}$ | $W_G$ | $E_B$ | $I_{rel}$ | $W_G$ | $E_B$ | $I_{rel}$ | $W_G$ | $E_B$ | $I_{rel}$ | $W_G$ |
| a | 531.41 | 88.44% | 1.28 | 531.49 | 82.38% | 1.28 | 531.62 | 82.86% | 1.16 | 531.60 | 80.02% | 1.18 |
| b | 533.59 | 11.56% | 1.93 | 533.55 | 17.62% | 1.93 | 533.53 | 17.14% | 1.56 | 533.59 | 19.98% | 1.65 |

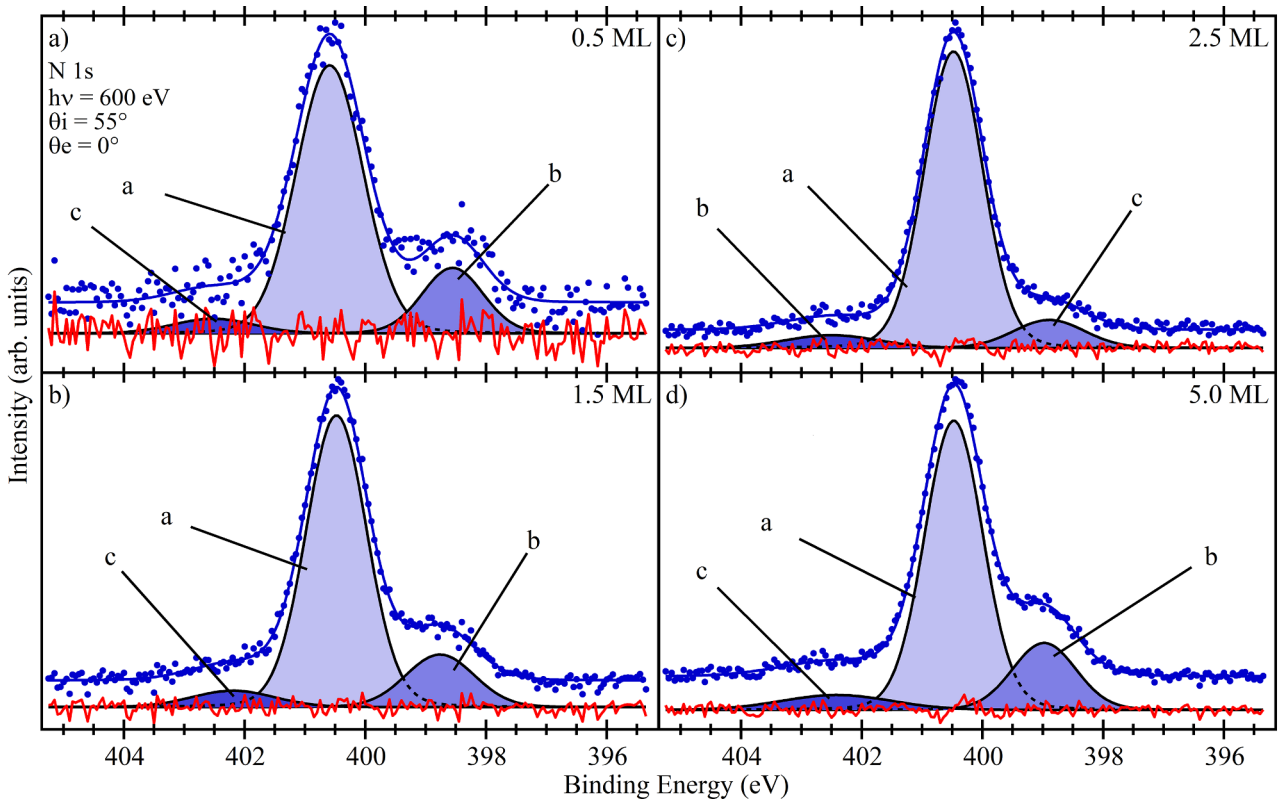


**Fig. 5.** Peakfits of N 1s core level spectra for four thicknesses of PTCDI on Sn/Si(111)-$2\sqrt{3} \times 2\sqrt{3}$. The measured data with Shirley background removed is plotted with blue dots. The result from the peakfit is plotted as a solid black line. Each fitted component is labelled as a–c and plotted with a filled, solid line. The residual is plotted as a solid red line.

is reasonable that it is the top Sn-atoms that interact with the molecules and hence 3/4 (75%) of the top Sn atoms are involved in the interaction. To understand the charge relaxation that results in the further reduction of *a* and increase of component *b* one would have to consider a more complex charge redistribution among the Sn atoms underneath. If the charge transfer to PTCDI happens from the top Sn atoms, it is possible that this also induces a charge redistribution among the Sn atoms in the first layer towards higher BE, which would explain the reduction of *a* and the increase of *b*.

The general behaviour of Sn-atoms losing charge in the interaction with PTCDI corresponds well with the results for C 1s core levels. Features involved in the C 1s core level spectra receiving charge in the molecule/substrate interaction move towards lower BE at low PTCDI coverages. The most drastic change in Fig. 3, is the strong depression of the imide related component *d* accompanied by the increase in intensity of the perylene-core related shakeup *e*. Comparing the relative intensities for these components at 0.5 and 5.0 ML it is clear that *d* loses about the same amount as *e* gains at low coverages. Considering the inverted behaviour of these two components, it is reasonable to assume that the imide related carbon receives charge in the interaction with the substrate and consequently shifts 1.4 eV to the energy position close to the shakeup *e*. Considering that component *e* is a mix of a shakeup and a partially shifted *d* component, it is generally hard to make any quantitative assertions using its relative intensity. Component *d*, on the other hand, has about 1/4 of its relative intensity at 0.5 ML compared to 5.0 ML. This would suggest that 75% of the carbons in the imide group receive charge from the Sn atoms in the interaction with the substrate.

At low coverages there is also a component *h* that is not needed at higher coverages, positioned at the high BE side of the main peak. This component has a relative intensity of 7.23% at 0.5 ML coverage and decreases in intensity quickly to the point where the component is barely needed to get a good fit at coverages above 1.5 ML. This would suggest that component *h* also is a component related to a molecule/substrate interaction. In earlier studies, this feature was found for submonolayer coverage of PTCDA on Sn-$2\sqrt{3}$, where it was suggested that it might be related to a shakeup feature from the perylene core [19]. On the other hand it was not found for PTCDI on Ag/Si(111)-$\sqrt{3} \times \sqrt{3}$ [20], henceforth Ag-$\sqrt{3}$, which would suggest that it could be due to an interaction between the perylene core of the molecules and the Sn-$2\sqrt{3}$ substrate.

Considering the BE position of *h*, it is reasonable that it is derived from the perylene core, rather than the imide group. Also, the difference in total relative intensity of components *a*–*c* at 0.5 ML (75.96%) and 5.0 ML (82.17%) is 6.2% which fits quite well with the 7.23% for

**Table 4**
Fitting parameters for the components used in the N 1s peakfit shown in Fig. 5. The table contains binding energy $E_B$ (eV), relative integrated intensity $I_{rel}$ and the FWHM ($W_G$) of the Gaussian (eV).

| | 0.5 ML | | | 1.5 ML | | | 2.5 ML | | | 5.0 ML | | |
|---|---|---|---|---|---|---|---|---|---|---|---|---|
| | $E_B$ | $I_{rel}$ | $W_G$ | $E_B$ | $I_{rel}$ | $W_G$ | $E_B$ | $I_{rel}$ | $W_G$ | $E_B$ | $I_{rel}$ | $W_G$ |
| a | 400.59 | 77.64 % | 1.25 | 400.45 | 78.14% | 1.13 | 400.48 | 84.57% | 1.09 | 400.48 | 74.06% | 1.08 |
| b | 398.55 | 17.39 % | 1.14 | 398.76 | 15.85% | 1.29 | 398.89 | 9.67% | 1.33 | 398.98 | 18.77% | 1.19 |
| c | 402.27 | 4.97 % | 1.52 | 402.19 | 6.01% | 1.58 | 402.24 | 5.76% | 1.77 | 402.41 | 7.17% | 2.12 |

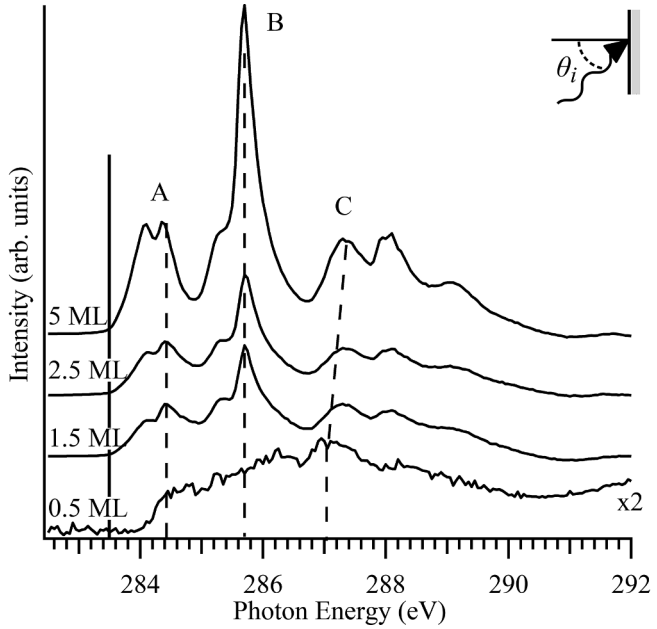


**Fig. 6.** C K-edge NEXAFS spectra of PTCDI on Sn/Si(111)-2$\sqrt{3}$ × 2$\sqrt{3}$ recorded at 70° incidence angle. The insert shows the incidence angle relative the sample normal.

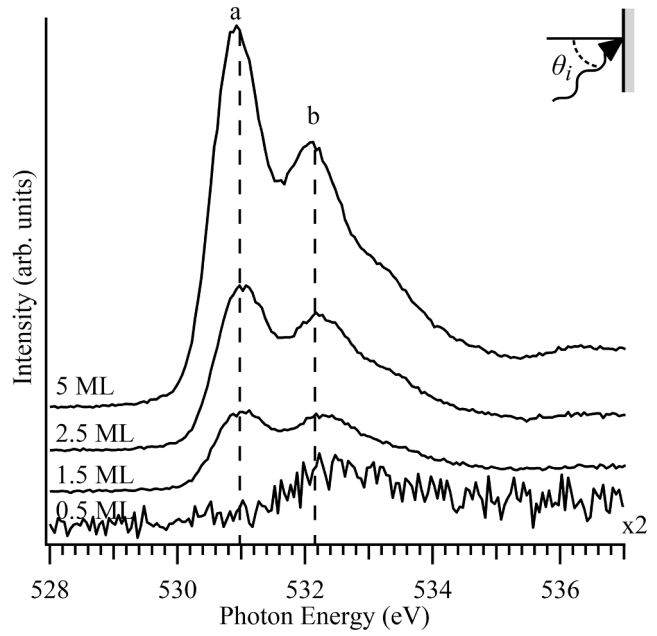


**Fig. 7.** O K-edge NEXAFS spectra of PTCDI on Sn/Si(111)-2$\sqrt{3}$ × 2$\sqrt{3}$ recorded at 70° incidence angle. The insert shows the incidence angle relative the sample normal.

component *h* at 0.5 ML PTCDI coverage. This would suggest that 2 carbon atoms per perylene core may be involved in this interaction. If component *h* is due to a part of the perylene core that is involved in the interaction it would mean that this particular part donates charge, as *h* is positioned at higher BE than the main peak. At a first glance, this does not fit with the behaviour of the Sn core levels of being shifted to higher BE positions. However, the Sn 4d component *b* does have a 0.16 eV shift towards lower BE when 0.5 ML PTCDI was evaporated onto the substrate. But considering the rather complex charge redistribution among the Sn atoms, it is impossible to conclude that the shift of the *b* component in Sn 4d is due to the interaction which would result in the C 1s component *h*.

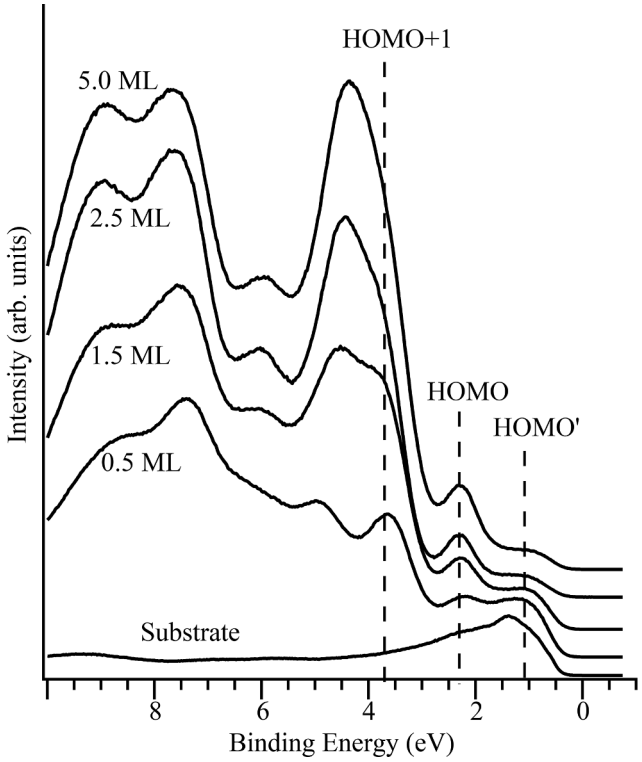


**Fig. 8.** Valence band spectra of PTCDI on Sn/Si(111)-2$\sqrt{3}$ × 2$\sqrt{3}$ recorded in normal emission, using a photon energy of 60 eV.

On the other hand, the interaction with the substrate shifts the perylene-core related main features towards lower BE, especially component *a* that shifts about 0.5 eV between 0.5 and 1.5 ML coverage. This would suggest that also the perylene core, mainly the carbon bond with hydrogen, receives charge in the interaction with the Sn-2$\sqrt{3}$ surface. Interestingly, the shift towards higher BE of the components in the perylene core does not saturate until a coverage of 2.5 ML. This is very similar to what is seen in the O 1s spectra, where the main peak shifts about 0.2 eV towards higher BE from 0.5 to 2.5 ML PTCDI coverage. Considering that the changes to the Sn 4d core levels are saturated between 0.5 and 1.5 ML, the shifts in the C 1s and O 1s core levels above 1.5 should therefore be attributed to intermolecular interactions rather than substrate/molecule interactions. It has been shown that PTCDI grows in island mode above 1 ML on Sn-2$\sqrt{3}$, and that molecules grow according to the canted structure within the layer of the islands [14]. For this reason, the intermolecular interactions are most likely C–H···O and N–H···O hydrogen bondings within each layer together with $\pi$–$\pi$ interactions between the layers [19].

The aforementioned shift for the main peak is the only change to the O 1s spectra, i. e. no large shifts or new components are found at low coverages. This is unexpected at first glance, considering the strong interaction between the substrate and the imide group which is revealed in the C 1s core levels, and the fact that an extra component in O 1s was found at submonolayer PTCDI coverages on the more weekly interacting substrate Ag-$\sqrt{3}$ [20]. However, the intensity shift from C 1s component *d* to *e* at low coverages has previously been observed for PTCDI on both Ag(111) and Cu(111). In neither of those cases could an extra component be found in the O 1s spectra but an extra component was found on the low BE side of the main peak in N 1s [4]. This is again similar to the situation found here for PTCDI on Sn-2$\sqrt{3}$, where the low BE component *b* is fairly strong at 0.5 ML coverage and loses relative intensity up to a coverage of 2.5 ML.

The changes in the N 1s core levels is especially interesting when comparing the results from the recent STM study of PTCDI on Sn-2$\sqrt{3}$ [14]. Up to coverages of about 0.5 ML, single molecules or rows of

molecules were found on the surface. The interaction between molecules in the most common rows were O···H–C hydrogen-bondings. This is in stark contrast to what is more commonly found, namely structures involving O···H–N hydrogen-bondings [21]. This makes this system unique considering that any interaction at coverages below 0.5 ML which involves the nitrogen atoms must be with the surface itself, not other molecules. It can therefore be definitely concluded that some of the nitrogen atoms do receive charge from the surface. In addition, O···H–C hydrogen bonding could cause the higher BE shift of the two neighboring carbon atoms, which may result in the component *h*.

The changes in the N 1s core level spectra need more discussions. At coverages between 0.5 and 1.0 ML, 2D structures started to form and several of these involve the O···H–N hydrogen-bondings. Also, above 1 ML new molecules that are adsorbed onto the surface can not interact with the substrate. These two factors together do explain why the low BE feature in the N 1s spectra is weakened with increasing PTCDI coverages. The increase of component *b* from 2.5 to 5.0 ML spectra is however unexpected. This change could in principle be due to intermolecular interactions between molecules in different layers, similarly to what was found for in the C and O 1s spectra at higher coverages, but this has not been found previously for high coverages of PTCDI on Au (111) or Ag-$\sqrt{3}$ [4,7].

Since the increase of the N 1s component *b* at high coverage cannot be due to molecule–substrate interaction, the difference in film morphology on the Ag-$\sqrt{3}$ and Sn-2$\sqrt{3}$ substrates must be considered. The STM studies of PTCDI on Ag-$\sqrt{3}$ and Sn-2$\sqrt{3}$ showed that the growth modes on the two surfaces are very different. On Ag-$\sqrt{3}$ the growth mode is layer-by-layer while island growth after the first ML is found on Sn-2$\sqrt{3}$ [7,20]. A morphology with high islands with a fairly small top area will have a significant amount of molecules sitting on the edges of the islands. These edge molecules will have missing intra layer interactions, i.e. they no longer participate in the typical N–H···O intra layer interaction. The molecules that are towards the edge will therefore have a different chemical environment and are likely to have a different inter layer interaction. For these reasons, we tentatively attribute the low BE N 1s component at high coverage as a charge effect due to the N···H bonding between different layers, which is enhanced by the special island growth mode.

The molecule/substrate interaction also affects the HOMO and LUMO levels, as seen in the UPS and NEXAFS spectra. All valence band spectra have a feature 2.3 eV below the Fermi level. This state is close to where the regular molecular HOMO for PTCDI has been found previously [7,18], and is also assigned as the HOMO on this surface. Interestingly, in the 0.5 ML spectrum there is another clear state above the HOMO level, denoted as HOMO' in Fig. 8, which is located at 1.1 eV below the Fermi level. The existence of the extra HOMO' state at low PTCDI coverages is accompanied by a complete removal of transitions to the first LUMO level in NEXAFS. This can be seen in the C K-edge spectra, but is most clearly seen in the O K-edge spectra where the first transition *a* is entirely gone at 0.5 ML coverage. At 1.5 ML the feature *a* is clearly visible, but its intensity is similar to that of feature *b* and with increasing PTCDI coverages *a* becomes the dominant feature.

Here it is interesting to compare the Sn-2$\sqrt{3}$ surface to the Ag-$\sqrt{3}$ surface. In the case of PTCDI on Ag-$\sqrt{3}$ the transitions to LUMO were severely weakened, but still visible at low coverages. Also, valence band spectra and scanning tunneling spectroscopy found four states around the Fermi level: One close to the regular HOMO level of PTCDI at 2.5 eV below the Fermi level (H), another filled state at 1.5 eV below the Fermi level (H'), a third filled state were found 0.3 eV below the Fermi level (L') and one empty state close to the regular LUMO level of PTCDI at 1 eV above the Fermi level (L). These states were then explained by a split of the HOMO and LUMO levels in combination with charge transfer: The HOMO–LUMO gap of the molecules is lowered due to the molecules interacting with the electric field from the Ag-$\sqrt{3}$ surface. Further, there are two types of molecules on the Ag-$\sqrt{3}$ surface due to molecules attaching to different adsorption sites. These two have different electronic configurations and hence different HOMO and LUMO levels. One type of molecules weakly receieve charge in the interaction and shift the energies level of the molecules to the point where its LUMO is filled and the frontier orbitals of this type is therefore H and L'. The frontier orbitals of the other type is H' and L. The existence of these two types of molecules could also be seen in STM where they had different contrast at certain biases [7,20,22].

For PTCDI on the Sn-2$\sqrt{3}$ surface there is a very different situation. In the STM investigation of this system, all molecules were found in the same adsorption geometries and the molecules did not have different contrast at any tunneling bias, so there was no clear evidence of two types of molecules. It was also found that the LUMO is located approximately 1.0 eV above the Fermi level [14]. Also, the core level data implies strong charge transfer from Sn, which directly involves the imide carbon and nitrogen, but not the oxygen atoms. On the Ag-$\sqrt{3}$ surface, all imide related features have an extra feature on the low BE side in carbon, oxygen and nitrogen core levels at low coverages. Further, the lack of transitions to the first LUMO level is found here for PTCDI on Sn-2$\sqrt{3}$. This, in combination with the existence of only one extra state in the valence band at low coverages, would suggest a splitting of the HOMO level, resulting in HOMO', and a lowering of the LUMO but again it is of a completely different nature than that for PTCDI on Ag-$\sqrt{3}$ where two extra states were found below the Fermi level.

A stronger interaction with the imide related carbon atoms and only one molecule configuration for the interaction on Sn-2$\sqrt{3}$ would also explain one big difference in the C 1s spectra when comparing with Ag-$\sqrt{3}$, namely the switch in intensity of component *d* and *e*. For PTCDI on Ag-$\sqrt{3}$ a partial shift from *d* to the position of component *e* was found where the two components had similar relative intensity at low coverages, which again was explained as only one of the type of molecules receiving charge [7]. Here on Sn-2$\sqrt{3}$ there is a more complete shift from *d* to *e*, but *d* still has about 25% of its relative intensity at low coverages compared to high. However, assuming that component *e* in the 0.5 ML spectrum mainly is the component *d* that has been shifted to lower BE one must also remember that this component has its own shakeup (*f* at higher coverages). The shakeup should be positioned about 1.3 eV above the imide related component. This means that component *d* at 0.5 ML to a large part should be considered as a shakeup component and consequently the shift from *d* to *e* as complete.

The changes due to the molecule/substrate interaction in the C 1s and O 1s spectra found in this work for PTCDI on Sn-2$\sqrt{3}$ are very similar to those for PTCDA on the same substrate [19]. This was to be expected considering that PTCDA [23,24] and PTCDI [14] had very similar adsorption geometries on Sn-2$\sqrt{3}$. However, PTCDA was found to have a stronger tendency to form 1D rows at low coverages and also formed larger patches of $4\sqrt{3} \times 2\sqrt{3}$ reconstruction. This would imply that PTCDA is slightly more mobile on the surface compared to PTCDI. At a first glance the C and O 1s core level spectra do not appear to support this. The two series of spectra show very similar behaviours for PTCDI and PTCDA on this substrate. Looking carefully, the three oxygen atoms in the carboxylic anhydride group are more electronegative than the two oxygen and the N–H in the imide counterpart, and hence the carbon atoms in the endgroup of PTCDA have slightly larger positive partial charge than the ones in PTCDI. Therefore the interaction found for both PTCDI and PTCDA on Sn-2$\sqrt{3}$, namely charge transfer from the substrate to carbon atoms in the endgroups, would be stronger for PTCDA rather than PTCDI. However, the N 1s core level spectra show that the nitrogen atoms are also involved in the interaction with the substrate, and the combination of charge transfer to the carbon and the nitrogen atoms in the endgroup of PTCDI could result in a overall stronger interaction with the substrate compared to PTCDA. Also, comparing the energy position of the extra state close to the Fermi level in the valence band spectra for the two molecules, they are located at 1.1 and 0.8 eV below the Fermi level for PTCDI and PTCDA respectively. The deeper position of this state for PTCDI indeed indicates a

stronger interaction between PTCDI compared to PTCDA and the Sn-$2\sqrt{3}$ surface.

## 5. Conclusions

The electronic structure of PTCDI on Sn/Si(111)-$2\sqrt{3} \times 2\sqrt{3}$ has been studied using high resolution XPS, UPS and NEXAFS. The results show a strong molecule/surface interaction which causes changes to the Sn 4d, C 1s and N 1s core level spectra. Also the HOMO and LUMO are modified as shown by VB and NEXAFS spectra. The interaction involves a charge transfer from the surface Sn atoms to the PTCDI molecules and in particular a significant charge donation to the imide carbon and partially to nitrogen atoms. This charge donation results in a splitting of the HOMO level and lowering of the LUMO level. This is seen in NEXAFS as missing resonance features and in the VB as an extra filled state (HOMO') at 1.1 eV. Thus our high resolution XPS, UPS, and NEXAFS data are in good agreement with the recent STM results.

## CRediT authorship contribution statement

**C. Emanuelsson:** Formal analysis, Investigation, Writing - original draft. **L.S.O. Johansson:** Conceptualization, Writing - review & editing, Supervision, Project administration, Funding acquisition. **H.M. Zhang:** Conceptualization, Investigation, Writing - review & editing, Supervision.

## Declaration of Competing Interest

The authors declare that they have no known competing financial interests or personal relationships that could have appeared to influence the work reported in this paper.

## Acknowledgments

The work done here was funded by the Swedish Research Council and the Tage Erlander foundation for science and technology.

## Appendix A. Supplementary data

Supplementary data associated with this article can be found, in the online version, at https://doi.org/10.1016/j.chemphys.2020.110973.

## References

[1] M. Carmen Ruiz Delgado, E.G. Kim, D.A. Da Silva Filho, J.L. Bredas, Tuning the charge-transport parameters of perylene diimide single crystals via end and/or core functionalization: A density functional theory investigation, Journal of the American Chemical Society 132 (10) (2010) 3375–3387, https://doi.org/10.1021/ja908173x.

[2] J. Taborski, P. Väterlein, H. Dietz, U. Zimmermann, E. Umbach, NEXAFS investigations on ordered adsorbate layers of large aromatic molecules, Journal of Electron Spectroscopy and Related Phenomena 75 (C) (1995) 129–147, https://doi.org/10.1016/0368-2048(95)02397-6.

[3] J.N. O'Shea, A. Saywell, G. Magnano, L.M.A. Perdigão, C.J. Satterley, P.H. Beton, V.R. Dhanak, Adsorption of PTCDI on Au(111): Photoemission and scanning tunnelling microscopy, Surface Science 603 (20) (2009) 3094–3098, https://doi.org/10.1016/j.susc.2009.08.024.

[4] A. Franco-Cañellas, Q. Wang, K. Broch, D.A. Duncan, P.K. Thakur, L. Liu, S. Kera, A. Gerlach, S. Duhm, F. Schreiber, Metal-organic interface functionalization via acceptor end groups: PTCDI on coinage metals, Physical Review Materials 1 (1) (2017) 013001, https://doi.org/10.1103/PhysRevMaterials.1.013001.

[5] G. Fratesi, V. Lanzilotto, S. Stranges, M. Alagia, G.P. Brivio, L. Floreano, High resolution NEXAFS of perylene and PTCDI: a surface science approach to molecular orbital analysis, Physical Chemistry Chemical Physics 16 (28) (2014) 14834, https://doi.org/10.1039/c4cp01625d.

[6] V. Lanzilotto, G. Lovat, G. Otero, L. Sanchez, G. Bavdek, L. Floreano, Commensurate growth of densely packed PTCDI islands on the rutile TiO 2 (110) surface, Journal of Physical Chemistry 117 (24) (2013) 12639–12647, https://doi.org/10.1021/jp402852u.

[7] C. Emanuelsson, L.S.O. Johansson, H.M. Zhang, Photoelectron spectroscopy studies of PTCDI on Ag/Si(111)–$\sqrt{3} \times \sqrt{3}$, The Journal of Chemical Physics 149 (4) (2018) 044702, https://doi.org/10.1063/1.5038721.

[8] C. Törnevik, M. Hammar, N.G. Nilsson, S.A. Flodström, Epitaxial growth of Sn on Si (111): A direct atomic-structure determination of the (2√3 × 2√3) R 30° reconstructed surface, Physical Review B 44 (23) (1991) 13144–13147, https://doi.org/10.1103/PhysRevB.44.13144.

[9] C. Törnevik, M. Göthelid, M. Hammar, U. Karlsson, N. Nilsson, S. Flodström, C. Wigren, M. Östling, Adsorption of Sn on Si(111)7 × 7: reconstructions in the monolayer regime, Surface Science 314 (2) (1994) 179–187, https://doi.org/10.1016/0039-6028(94)90005-1.

[10] L. Ottaviano, G. Profeta, L. Petaccia, C. Nacci, S. Santucci, Structural and electronic properties of the Sn/Si(111)-($2\sqrt{3} \times 2\sqrt{3}$)R30 surface revised, Surface Science 554 (2–3) (2004) 109–118, https://doi.org/10.1016/j.susc.2004.02.019.

[11] P.E.J. Eriksson, J.R. Osiecki, K. Sakamoto, R.I.G. Uhrberg, Atomic and electronic structures of the ordered $2\sqrt{3} \times 2\sqrt{3}$ and molten 1 × 1 phase on the Si(111): Sn surface, Physical Review B 81 (23) (2010) 235410, https://doi.org/10.1103/PhysRevB.81.235410.

[12] Y. Sugimoto, M. Abe, S. Hirayama, S. Morita, Highly resolved non-contact atomic force microscopy images of the Sn/Si(111)-($2\sqrt{3} \times 2\sqrt{3}$) surface, Nanotechnology 17 (16) (2006) 4235–4239, https://doi.org/10.1088/0957-4484/17/16/039.

[13] H.M. Zhang, J.B. Gustafsson, L.S.O. Johansson, Electronic structure of PTCDA on Sn/Si(111)-√3 x √3, Physical Review B 84 (20) (2011) 8, https://doi.org/10.1103/PhysRevB.84.205420.

[14] C. Emanuelsson, M.A. Soldemo, L.S.O. Johansson, H.M. Zhang, Scanning tunneling microscopy study of PTCDI on Sn/Si(111)-2√3 × 2√3, The Journal of Chemical Physics 150 (4) (2019) 044709, https://doi.org/10.1063/1.5070120.

[15] R. Nyholm, J.N. Andersen, U. Johansson, B.N. Jensen, I. Lindau, Beamline I311 at MAX-LAB: A VUV/soft X-ray undulator beamline for high resolution electron spectroscopy, Nuclear Instruments and Methods in Physics Research, Section A: Accelerators, Spectrometers, Detectors and Associated Equipment 467–468 (2001) 520–524, https://doi.org/10.1016/S0168-9002(01)00399-0.

[16] A. Ishizaka, Y. Shiraki, Low temperature surface cleaning of silicon and its application to silicon MBE, Journal of The Electrochemical Society 133 (4) (1986) 666, https://doi.org/10.1149/1.2108651.

[17] D.R.T. Zahn, G.N. Gavrila, G. Salvan, Electronic and vibrational spectroscopies applied to organic/inorganic interfaces, Chemical Reviews 107 (4) (2007) 1161–1232, https://doi.org/10.1021/cr050141p.

[18] D.R.T. Zahn, G.N. Gavrila, M. Gorgoi, The transport gap of organic semiconductors studied using the combination of direct and inverse photoemission, Chemical Physics 325 (1) (2006) 99–112, https://doi.org/10.1016/j.chemphys.2006.02.003.

[19] H. Zhang, L. Johansson, Electronic structure of PTCDA on Sn/Si(111)-$2\sqrt{3} \times 2\sqrt{3}$, Chemical Physics 439 (2014) 71–78, https://doi.org/10.1016/j.chemphys.2014.05.013.

[20] C. Emanuelsson, H.M. Zhang, E. Moons, L.S.O. Johansson, Scanning tunneling microscopy study of thin PTCDI films on Ag/Si(111)-$\sqrt{3} \times \sqrt{3}$, Journal of Chemical Physics 146 (11) (2017).

[21] M. Mura, F. Silly, G.A.D. Briggs, M.R. Castell, L.N. Kantorovich, H-bonding supramolecular assemblies of PTCDI molecules on the Au(111) surface, Journal of Physical Chemistry C 113 (52) (2009) 21840–21848, https://doi.org/10.1021/jp908046t.

[22] C. Emanuelsson, L.S.O. Johansson, H.M. Zhang, Delicate interactions of PTCDI molecules on Ag/Si(111)-√3 × √3, The Journal of Chemical Physics 149 (16) (2018) 164707, https://doi.org/10.1063/1.5053606.

[23] H.M. Zhang, L.S.O. Johansson, STM study of PTCDA on Sn/Si(111)-2√3 × 2√3, The Journal of Chemical Physics 144 (12) (2016) 124701, https://doi.org/10.1063/1.4944389.

[24] N. Nicoara, Z. Wei, J.M. Gómez-Rodríguez, One-dimensional growth of PTCDA molecular rows on Si(111)-($2\sqrt{3} \times 2\sqrt{3}$)R30 -Sn surfaces, The Journal of Physical Chemistry C 113 (33) (2009) 14935–14940, https://doi.org/10.1021/jp904051h.